First-principles study of the thermal expansion of Be$(10\bar{1}0)$

Michele Lazzeri[1,2,*] and Stefano de Gironcoli[2]
[1]*Department of Chemistry, Princeton University, Princeton, New Jersey 08540*
[2]*INFM and Scuola Internazionale Superiore di Studi Avanzati (SISSA), via Beirut 2-4, I-34014 Trieste, Italy*
(Received 30 August 2001; revised manuscript received 8 March 2002; published 28 May 2002)

We present a first-principles study of the thermal expansion of Be$(10\bar{1}0)$ surface, within the quasiharmonic approximation (QHA). The maximum temperature studied ($T=700$ K) is well below melting and QHA is adequate in this regime. Many layers are involved in the thermal relaxation of this surface, and in order to apply QHA to this complex system we developed a method for the efficient computation of the third-order derivatives of the total energy in a metallic system using the density-functional perturbation theory . Computer codes for this method are made available on the web. We find that as the temperature increases the short interlayer spacings near the surface contract and the long interlayer spacings expand. The mechanism leading to this behavior is disclosed and compared with that for Mg$(10\bar{1}0)$ and Al(110) surfaces, where a similar effect was previously observed.

DOI: 10.1103/PhysRevB.65.245402 PACS number(s): 68.35.Bs, 65.40.De, 68.35.Ja, 71.15.Mb

I. INTRODUCTION

Thermal expansion of low index metallic surfaces can lead to a rich variety of behaviors for different systems, and, through the years, this topic has attracted both experimental and theoretical attention. Particularly interesting is the recent discovery of systems in which the distance between the first two surface atomic layers decreases by increasing the temperature (*thermal contraction*). This phenomenon was first observed in the Al(110) surface by measurements[1] and first-principles calculation,[2] and then in the Mg$(10\bar{1}0)$ surface.[3] In the latter case both measurements and calculations reported an oscillatory thermal expansion, i.e., contraction of the first and third interlayer spacing, and expansion of the second and fourth interlayer spacing.

In a purely harmonic crystal atomic mean positions do not change by increasing the temperature, thus, thermal expansion is a consequence of anharmonic terms in the interatomic potential. The occurrence of the first interlayer thermal contraction in Al(110) is explained by Marzari *et al.*[2] as the consequence of the larger anharmonicity of the second surface layer with respect to the first one. On the contrary, on Mg$(10\bar{1}0)$ thermal contraction is strictly linked to the increase of the bulk lattice spacing parallel to the surface.[3] At a given temperature, the mean position of atomic surface layers is determined by the balance between energetic and entropic effects, and from general arguments one should expect a surface to expand by increasing the temperature.[4] Indeed, in both Al(110), and Mg$(10\bar{1}0)$ surfaces the surface as a whole expands. Hence, interlayer thermal contraction is a topic deserving much attention in view of a better understanding of the delicate interplay between energetic and entropic effects at the surface.

Nowadays, there are essentially two feasible methods to treat thermal expansion within a computational approach based on density-functional theory:[5] molecular-dynamics (MD) simulation and lattice dynamics in the quasiharmonic approximation (QHA). These are two complementary approaches: while MD is valid only above the Debye temperature, where quantum effects are negligible, the QHA is valid well below the melting temperature. QHA is commonly believed to describe correctly bulk properties. It has also been used to describe surface thermal expansion for several systems,[6–8] although the surface case is more delicate and special care should be used in applying the QHA scheme to it. An accurate representation of the density of vibrational states is necessary in order to obtain the quasiharmonic free energy,[9] and oversimplified approaches can be misleading, as we demonstrated in the case of Be(0001) surface.[7] Moreover, for Al(100) (Ref. 10) and Ag(111) (Ref. 11) it was shown that QHA is inadequate to describe surface thermal expansion for temperature approaching melting.

The density-functional perturbation theory (DFPT) approach of Ref. 12 allows the efficient computation of the vibrational frequencies, which are necessary in order to calculate the Helmholtz free energy within the QHA. However, because of the complexity of the calculations involved, up to now the QHA has been used to study surfaces in which essentially only one layer is involved in the thermal expansion.[6–8] Application of the method to more complex systems requires the knowledge not only of the vibrational frequencies of a system but also of their derivatives with respect to atomic displacements. These quantities are related to the third-order derivatives of the total energy of the system. In this work we will describe an efficient algorithm to compute third-order derivatives of the total energy within the DFPT approach, extending the so-called "$2n+1$" theorem[13] to metallic systems.

In a recent work,[3] this approach already allowed us to describe, within QHA, the complex pattern of multilayer thermal expansion in Mg$(10\bar{1}0)$ surface. Our calculations, performed in an appropriate range of temperature, resulted in good agreement with low electron energy diffraction measurements.[3] In this work we will use the same method to study the thermal expansion of Be$(10\bar{1}0)$ surface up to the temperature $T=700$ K, which is well below bulk Be melting temperature (~ 1600 K). On Be$(10\bar{1}0)$ surface we observe an oscillatory thermal relaxation similar to and stronger than

the one we have previously reported for Mg($10\bar{1}0$). The mechanism leading to this phenomenon will be analyzed, pointing out similarity and differences of the two systems.

The outline of the paper is as follows. In Sec. II we briefly summarize the QHA approach and we describe a general method to calculate the third-order derivatives of the total energy in a metallic system. In Sec. III we give more technical details about the calculation, and we present the obtained thermal expansion of Be($10\bar{1}0$) surface. Finally, in Sec. IV we analyze the results, making a comparison with Mg($10\bar{1}0$) and Al(110) surfaces.

II. METHOD

A. The quasiharmonic approximation

Let us consider a crystal described by the structural parameters $\mathbf{p}=(p_1,p_2,\ldots,p_n)$. In the QHA the Helmholtz free energy F is approximated by

$$F(T,\mathbf{p})=E^{tot}(\mathbf{p})+F^{vib}(T,\mathbf{p}) \tag{1}$$

$$=E^{tot}(\mathbf{p})+k_BT\sum_{\alpha}\ln\left[2\sinh\left[\frac{\hbar\omega_{\alpha}(\mathbf{p})}{2k_BT}\right]\right],$$

where $E^{tot}(\mathbf{p})$ is the total static energy of the crystal and $\omega_{\alpha}(\mathbf{p})$ are the frequencies of the vibrational modes. Given a temperature T, the equilibrium values of the parameters $\mathbf{p}$ are obtained by minimizing F. If the system is described by one or two parameters only it is practical and efficient to compute $\omega_{\alpha}(\mathbf{p})$ in various points in the parameter space, calculate F^{vib} exactly in these points, and interpolate its value in between when searching the minimum. In the general case this scheme is cumbersome, and a simpler approach, if the needed derivatives are available, is to solve directly the system of equations

$$\frac{\partial E^{tot}}{\partial p_i}(\mathbf{p})+\frac{\partial F^{vib}}{\partial p_i}(\mathbf{p},T)=0, \tag{2}$$

by any of the methods used in structural optimization. The computation of the derivatives of the vibrational contribution to the free energy is, however, at least one order of magnitude more complex than the first term in Eq. (2). For surfaces, thus, the slightly different approach described below is more appropriate.

The structure of a surface is defined by the positions of the surface layers ($\mathbf{d}=d_1,d_2,\ldots$) and the bulk parameters $\mathbf{a}$, which in an hcp crystal are the two lattice parameters $\mathbf{a}=(a,c)$. Before approaching the surface problem, the dependence on T of the bulk parameters $[\mathbf{a}(T)]$ can be obtained by an independent calculation. Afterward, as a first approximation, one can assume a linear dependence of F^{vib} on $\mathbf{d}$. In this hypothesis the derivatives of the vibrational contribution to the free energy , $-(\partial F^{vib}/\partial d_i)$, [we will call them vibrational forces (VF's)] do not depend on $\mathbf{d}$, and the system of equations to be solved is

$$\frac{\partial E^{tot}}{\partial d_i}[\mathbf{a}(T),\mathbf{d}]+\frac{\partial F^{vib}}{\partial d_i}[\mathbf{a}(T),T]=0, \tag{3}$$

where the static forces, $-\partial E^{tot}/\partial d_i(\mathbf{d})$, can be efficiently calculated for any point in the configuration space of $\mathbf{d}$ thanks to Hellmann-Feynman theorem. The solution of Eq. (3) is not more complex than a standard structural relaxation and provides an estimate of the equilibrium parameters of the system. An improved solution, to any desired accuracy level, can be obtained by calculating the VF's for the new configuration and iterating the procedure to self consistency.

The VF's in a crystal depend on the vibrational frequencies ω_{α} and on their derivatives $\partial\omega_{\alpha}/\partial d_i$ which, in turn, can be obtained from the second- and third-order derivatives of the total energy of the system with respect to distortions of the atomic geometry. In the remaining of this section we will describe the *first-principles* approach that we used to calculate second- and third-order derivatives of the energy. We will give the expression for the energy derivatives with respect to a generic parameter, from which ω_{α} and $\partial\omega_{\alpha}/\partial d_i$ can be easily obtained as explained in Refs. 12,13.

B. First-principles approach

We used a plane-wave and pseudopotential approach to the density-functional theory (DFT) of Ref. 5. Within DFT, derivatives of the total energy can be obtained thanks to the "$2n+1$" theorem.[13] In this context the theorem states that, given the nth-order variation of the electronic charge density with respect to an external perturbation, it is possible, in principle, to obtain the variation of the total energy up to the $(2n+1)$th order. As a consequence, the first-order variation of the charge density gives access to second- and third-order derivatives of the energy. First-order variation of the charge can be obtained by linear-response methods such as DFPT,[12] and its generalization to metals.[14] DFPT has already allowed third-order calculations in semiconducting systems,[15,16] and in the following sections this scheme is extended to the more complex metallic case. As a first step, in the following section, we rewrite the metallic DFPT in a slightly different way from that reported in Ref. 14.

C. Linear response for metals

In a metallic system a large number of k points is necessary to reach sufficient accuracy in the Brillouin-zone sampling. A commonly used approach to this problem is to introduce a smearing function $\tilde{\theta}(x)$,[17] that is an approximation of the step function characterized by a smearing width σ. The only justification for this *ad hoc* procedure is that as $\sigma\rightarrow 0$ one would recover the "absolutely" converged result (at the expense of using a prohibitively fine k-point mesh), and that, even at a finite value of σ, one can obtain accurate results.

Within the smearing approach, the Kohn-Sham (KS) equations, which are to be solved self-consistently to obtain the electronic charge density $n(\mathbf{r})$, are

$$[T^{kin}+V_{KS}]|\psi_i\rangle=\epsilon_i|\psi_i\rangle, \tag{4}$$

$$V_{KS}(\mathbf{r})=v_{ext}(\mathbf{r})+\frac{\delta E_I[n]}{\delta n(\mathbf{r})}, \tag{5}$$

$$n(\mathbf{r})=\sum_i \tilde{\theta}_{Fi}|\psi_i(\mathbf{r})|^2, \tag{6}$$

$$\sum_i \tilde{\theta}_{Fi}=\int n(\mathbf{r})d\mathbf{r}=N, \tag{7}$$

where T^{kin} is the single-particle kinetic-energy operator, V_{KS} is the self-consistent KS potential, v_{ext} is the external potential due to the ions, $E_I[n]$ is the interaction functional (usually written as the sum of the Hartree energy and an exchange-correlation contribution), N is the number of electrons, and $\tilde{\theta}_{Fi}=\tilde{\theta}(\epsilon_F-\epsilon_i)$, where the Fermi energy ϵ_F is determined by the last equation. The natural definition of the total electronic energy becomes[14]

$$E_v[n]=\sum_i \{\tilde{\Delta}_{Fi}+\epsilon_i\tilde{\theta}_{Fi}\}+\left\{E_I[n]-\int\frac{\delta E_I[n]}{\delta n(\mathbf{r})}n(\mathbf{r})d\mathbf{r}\right\}, \tag{8}$$

where $\tilde{\Delta}_{Fi}=\int_{-\infty}^{x}y\tilde{\delta}(y)dy|_{x=\epsilon_F-\epsilon_i}$, and $\tilde{\delta}(x)=(\partial/\partial x)\tilde{\theta}$.

When a perturbation $\lambda v_{ext}^{(1)}$ is superimposed on the external potential, the KS self-consistent potential is modified accordingly to $V_{KS}\rightarrow V_{KS}+\lambda V_{KS}^{(1)}$, where λ is a small parameter. We will indicate the nth derivative of a quantity F, with respect to λ equivalently by $F^{(n)}$ or $(d^n/d\lambda^n)F$. It is convenient to introduce a "cutoff" energy $\bar{E}$ that separates the electronic states that are partially occupied due to the finite width of the smearing function from those that can be considered completely empty. In practice one can choose any $\bar{E}\geqslant\epsilon_F+3\sigma$, where σ is the width of the smearing function $\tilde{\theta}$. The first variation of the charge density $n^{(1)}(\mathbf{r})$ can then be obtained solving self-consistently the following set of equations:

$$[T^{kin}+V_{KS}+\alpha P_v^-\epsilon_i]\ |\phi_i\rangle=-P_c^-V_{KS}^{(1)}|\psi_i\rangle, \tag{9}$$

$$V_{KS}^{(1)}(\mathbf{r})=v_{ext}^{(1)}(\mathbf{r})+\int\frac{\delta^2E_I[n]}{\delta n(\mathbf{r})\delta n(\mathbf{r}')}n^{(1)}(\mathbf{r}')d\mathbf{r}', \tag{10}$$

$$n^{(1)}(\mathbf{r})=\sum_i^{\bar{v}}\{\tilde{\theta}_{Fi}[\phi_i(\mathbf{r})\psi_i^*(\mathbf{r})+cc]+\tilde{\delta}_{Fi}\epsilon_F^{(1)}|\psi_i(\mathbf{r})|^2\},$$
$$+\sum_{ij}^{\bar{v}}\frac{\tilde{\theta}_{Fi}-\tilde{\theta}_{Fj}}{\epsilon_i-\epsilon_j}\psi_j(\mathbf{r})\langle\psi_j|V_{KS}^{(1)}|\psi_i\rangle\psi_i^*(\mathbf{r}), \tag{11}$$

where $\tilde{\delta}_{Fi}=\tilde{\delta}(\epsilon_F-\epsilon_i)$, $\Sigma^{\bar{v}}$ indicates summation over the partially occupied states (those with energy $\leqslant\bar{E}$), P_v^- is a projector on the manifold spanned by these states, while $P_c^-=1-P_v^-$ is the projector on the empty-state manifold. Equation (9) needs to be solved only for the partially occupied states, and the value of α must be chosen so that the linear system is not singular. It can be demonstrated that $|\phi_i\rangle=P_c^-|\psi_i^{(1)}\rangle$, where $|\psi_i^{(1)}\rangle$ is the first-order variation of a wave function, which in standard perturbation theory is given by

$$|\psi_i^{(1)}\rangle=\sum_{\epsilon_j\neq\epsilon_i}|\psi_j\rangle\frac{\langle\psi_j|V_{KS}^{(1)}|\psi_i\rangle}{\epsilon_i-\epsilon_j}. \tag{12}$$

D. Third order for metals

Taking the third-order derivative of Eq. (8) with respect to λ one obtains

$$E_v^{(3)}=\sum_i\left\{\left(\frac{d^2}{d\lambda^2}\tilde{\theta}_{Fi}\right)\epsilon_i^{(1)}+2\left(\frac{d}{d\lambda}\tilde{\theta}_{Fi}\right)\epsilon_i^{(2)}+\tilde{\theta}_{Fi}\epsilon_i^{(3)}\right\}$$
$$+\frac{d^3}{d\lambda^3}\left\{E_I[n]-\int\frac{\delta E_I[n]}{\delta n(\mathbf{r})}n(\mathbf{r})d\mathbf{r}\right\}, \tag{13}$$

that, following Ref. 13, can be reduced to

$$E_v^{(3)}=Z+\int v_{ext}^{(3)}(\mathbf{r})n(\mathbf{r})d\mathbf{r}+3\int v_{ext}^{(2)}(\mathbf{r})n^{(1)}(\mathbf{r})d\mathbf{r}$$
$$+\int\frac{\delta^3E_I[n]}{\delta n(\mathbf{r})\delta n(\mathbf{r}')\delta n(\mathbf{r}'')}n^{(1)}$$
$$\times(\mathbf{r})n^{(1)}(\mathbf{r}')n^{(1)}(\mathbf{r}'')d\mathbf{r}d\mathbf{r}'d\mathbf{r}'', \tag{14}$$

with

$$Z=\sum_i\left\{6\tilde{\theta}_{Fi}\langle\psi_i^{(1)}|V_{KS}^{(1)}-\epsilon_i^{(1)}|\psi_i^{(1)}\rangle+\tilde{\delta}_{Fi}^{(1)}(\epsilon_i^{(1)}-\epsilon_F^{(1)})^3\right.$$
$$\left.+6\left(\frac{d}{d\lambda}\tilde{\theta}_{Fi}\right)\langle\psi_i|V_{KS}^{(1)}|\psi_i^{(1)}\rangle\right\}, \tag{15}$$

where $\tilde{\delta}_{Fi}^{(1)}=(\partial/\partial x)\tilde{\delta}|_{\epsilon_F-\epsilon_i}$. In the present form the term Z cannot be easily computed. Both conduction and valence states are, in fact, required to calculate $|\psi_i^{(1)}\rangle$. Moreover, the possibility that the denominator in Eq. (12) approaches zero may lead to numerical instabilities. For semiconductors these problems can be overcome following the recipe given in Refs. 15,16. However, that approach is based on the existence of an energy gap between occupied and unoccupied states, and is not useful for metals.

To deal with the metallic case, we rewrite Z as

$$Z=6\sum_i\tilde{\theta}_{Fi}\langle\phi_i|V_{KS}^{(1)}|\phi_i\rangle$$
$$+6\sum_{ij}^{\bar{v}}\frac{\tilde{\theta}_{Fi}\langle\phi_i|V_{KS}^{(1)}|\psi_j\rangle V_{ji}^{(1)}-\tilde{\theta}_{Fj}\langle\psi_i|V_{KS}^{(1)}|\phi_j\rangle V_{ji}^{(1)}}{\epsilon_{ij}}$$
$$+2\sum_{ijk}^{\bar{v}}\frac{V_{ij}^{(1)}V_{jk}^{(1)}V_{ki}^{(1)}}{\epsilon_{ij}\epsilon_{jk}\epsilon_{ki}}(\tilde{\theta}_{Fi}\epsilon_{kj}+\tilde{\theta}_{Fk}\epsilon_{ji}+\tilde{\theta}_{Fj}\epsilon_{ik})$$
$$+3\epsilon_F^{(1)}\left\{\sum_{ij}^{\bar{v}}\frac{\tilde{\delta}_{Fi}-\tilde{\delta}_{Fj}}{\epsilon_{ij}}V_{ij}^{(1)}V_{ji}^{(1)}+2\sum_i\tilde{\delta}_{Fi}\langle\psi_i|V_{KS}^{(1)}|\phi_i\rangle\right\}$$
$$+3(\epsilon_F^{(1)})^2\left(\sum_i\tilde{\delta}_{Fi}^{(1)}V_{ii}^{(1)}\right)-(\epsilon_F^{(1)})^3\left(\sum_i\tilde{\delta}_{Fi}^{(1)}\right), \tag{16}$$

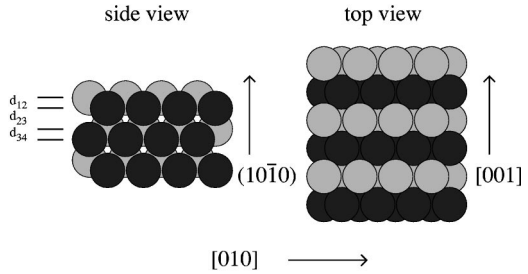

FIG. 1. Schematic drawing of the *hcp* Be$(10\bar{1}0)$ surface. d_{ij} indicates the separation between the ith and jth surface layers. Atoms with different color belong to different (0001) planes.

where $V_{ij}^{(1)}=\langle\psi_i|V_{KS}^{(1)}|\psi_j\rangle$, $\epsilon_{ij}=\epsilon_i-\epsilon_j$, and $|\phi_i\rangle$ can be obtained from Eq. (9). In this way, we have expressed the third-order derivative of the energy of a metallic system in a form that depends only on the finite number of partially occupied eigenstates of the KS Hamiltonian. Furthermore, every term in Eq. (16) having a (nearly) null denominator has a well-defined and finite limit that can be explicitly computed. As an example

$$\lim_{\epsilon_i\to\epsilon_j}\frac{\tilde{\theta}_{Fi}\langle\phi_i|V_{KS}^{(1)}|\psi_j\rangle V_{ji}^{(1)}-\tilde{\theta}_{Fj}\langle\psi_i|V_{KS}^{(1)}|\phi_j\rangle V_{ji}^{(1)}}{\epsilon_{ij}}=$$

$$-\tilde{\theta}_{Fi}\langle\phi_i|\phi_j\rangle V_{ji}^{(1)}-\tilde{\delta}_{Fi}\langle\psi_i|V_{KS}^{(1)}|\phi_j\rangle V_{ji}^{(1)}. \qquad (17)$$

A code implementing the concepts above has been developed in the framework of the PWSCF and PHONON package,[18] and is available on the web at the same URL.

III. Be$(10\bar{1}0)$ SURFACE

A. Technical details

Calculations were performed within the local-density approximation,[19] using separable pseudopotentials,[20] and including nonlinear core correction.[21] Brillouin-zone integrations were performed within the smearing approach of Ref. 17, using the Hermite-Gauss smearing function of order one. In two previous works[22,23] we demonstrated that this approach reproduces correctly the low-temperature structural and vibrational properties of Be bulk and its (0001) and $(10\bar{1}0)$ surfaces. Furthermore, in Ref. 7 we showed that QHA correctly reproduces Be bulk thermal expansion up to the temperature $T=700$ K. A direct comparison with a first-priciples molecular-dynamics run established its validity on the (0001) surface up to this temperature. Details of the present work are the same as in Refs. 7,22,23.

B. Static-equilibrium structure

We obtained the static-equilibrium structure of the Be bulk and of Be$(10\bar{1}0)$ surface by minimizing the total energy.[22,23] Calculated equilibrium *hcp* lattice constants are in good agreement with experimental values (in parentheses): $a=4.25$ (4.33) a.u., $c/a=1.572$ (1.568). The structure of the *hcp* Be$(10\bar{1}0)$ surface is depicted in Fig. 1. In an *hcp* crystal, the distance d between two neighboring atomic layers parallel to the $(10\bar{1}0)$ surface has two possible values $d=a/\sqrt{3}$, or $d=0.5a/\sqrt{3}$. We will call them long- and short-interlayer distance, respectively. $(10\bar{1}0)$ surface can be terminated in two possible ways, depending on whether the first surface interlayer distance is ''short,'' or ''long.'' For this work we have considered only the most stable[24] ''short'' termination. The surface relaxation we obtained is compared in Table I with the results previously obtained for the Mg$(10\bar{1}0)$ surface.[3] Although results reported in Table I are obtained by a purely static relaxation and do not include zero-point energy effects, they are in reasonable agreement with low-temperature low-energy electron-diffraction (LEED) measurements.[24,3] Indeed, we will show in the following section that zero-point energy does not considerably affect low-temperature surface relaxation.

TABLE I. Static relaxation of Be and Mg$(10\bar{1}0)$ surfaces. Δd_{ij} is the difference from the corresponding bulk value of the distance between ith and jth surface layers.

	Be$(10\bar{1}0)$		Mg$(10\bar{1}0)$	
	Calc.[a]	Expt.[b]	Calc.[c]	Expt.[d]
$\Delta d_{12}(\%)$	-24.5	$-25(-4/+3)$	-19.0	-16.4 ± 2.0
$\Delta d_{23}(\%)$	$+6.6$	$+5(-3/+5)$	$+7.9$	$+7.8\pm1.0$
$\Delta d_{34}(\%)$	-14.8	$-11(-5/+8)$	-10.8	-10.5 ± 3.0
$\Delta d_{45}(\%)$	$+4.7$	$+2(-2/+4)$	$+3.9$	$+3.8\pm1.6$
$\Delta d_{13}(\%)$	-3.8	-5.0	-1.1	-0.3
$\Delta d_{24}(\%)$	-0.5	-0.3	$+1.7$	$+1.7$
$\Delta d_{35}(\%)$	-1.8	-2.3	-1.0	-1.0
$\Delta d_{46}(\%)$	$+0.6$		$+1.0$	$+0.7$

[a]Calculation from Ref. 23.
[b]Experimental from Ref. 24.
[c]Calculation from Ref. 3.
[d]Experimental from Ref. 3.

In both Be and Mg the surface undergoes an oscillatory relaxation consisting in a contraction of the ''short'' spacings (the first and the third surface interlayer distances), and an expansion of the ''long'' spacings (the second and the fourth). From Table I we can also notice that in both cases the sum of a ''short'' and a ''long'' spacing (i.e. $d_{n,n+2}$, where d_{ij} is the distance between the ith and the jth layers) relax by a lower percentage than a single interlayer spacing ($d_{n,n+1}$), suggesting that the contraction of the ''short'' spacing is intimately tied with the expansion of the ''long'' one. The relaxation of the two surfaces is thus very similar despite the fact that Be and Mg have very different bulk and surface electronic structures.[25] This suggests that the geometry of the *hcp* $(10\bar{1}0)$ surface plays an important role. A possible way of interpreting these relaxation patterns, which relies essentially on the structure of the $(10\bar{1}0)$ surface, is described in the remaining of this section. A similar argument was already used by Narasimhan to explain structural features of some *fcc* (110) surfaces.[26]

Let us call $\Phi_{n,m}$ the second derivative of the energy with respect to displacements, perpendicular to the $(10\bar{1}0)$ surface, of the nth and mth layers. According to our calculations in bulk Be $\Phi_{n,n+1}=-0.031$ or -0.022 a.u. (there are two inequivalent possibilities), and $\Phi_{n,n+2}=-0.036$ a.u.. In bulk Mg, $\Phi_{n,n+1}=-0.010$ or -0.003 a.u. and $\Phi_{n,n+2}=-0.022$ a.u. In both cases $|\Phi_{n,n+2}|$ is larger than $|\Phi_{n,n+1}|$, implying that a displacement of the nth layer will induce a stronger force on the $(n+2)$th layer than on the $(n+1)$th one. This is not surprising: in an *hcp* crystal, atoms are arranged in planes in the (0001) direction (see Fig. 1) and bonds between nearest-neighbor (NN) atoms connect the nth $(10\bar{1}0)$ surface layer not only with the $(n+1)$th layer but also with the $(n+2)$th one. In fact, the bonds between NN atoms belonging to the nth and $(n+1)$th layers form a lower angle with the surface than the bonds between NN's belonging to nth and $(n+2)$th layers. Thus the atomic motion in the surface normal direction stretches more the bond length with NN's in $(n+2)$th layer than with those in $(n+1)$th layer. If the interlayer potential between the nth and $(n+1)$th layers is softer than the one between nth and $(n+2)$th ones, it is easier to change the distances between the 1st and 2nd, 3rd and 4th, . . . layers, than between 1st, 3rd, 5th, . . . layers. When this is the case, a contraction of the first interlayer spacing will induce an expansion of the second interlayer spacing and an oscillatory relaxation of the lower layers, just as observed in Be and Mg $(10\bar{1}0)$ surfaces.

The contraction of the first interlayer spacing in a metallic surface is not an unusual behavior: surface atoms move toward the bulk so as to increase their coordination and increase the density of the surrounding charge.[27] We suggest that the relative stiffness of surface layers explains how the contraction of the first interlayer propagates to the lower layers in an oscillatory way.

C. Thermal expansion

In order to calculate the VF's (defined in Sec. II A), which are necessary to obtain the thermal expansion, we calculated the dynamical matrices of a 16-layers slab and their derivatives with respect to atomic displacements. These matrices were calculated exactly at two different sets of in-plane spacings corresponding to the static-equilibrium structure and to the theoretical bulk value at $T=700$ K. The matrices used for the intermediate temperatures were obtained by linear interpolation. The vibrational free energy and VF's of the five outermost layers were calculated summing over a 10×10 grid in the surface Brillouin zone and over all the branches of a slab obtained Fourier interpolating matrices calculated exactly on a 2×2 grid. As a first approximation, we calculated VF's using slabs having the layers in the positions corresponding to the static equilibrium.

In order to solve Eq. (3) we relaxed the atomic positions (by minimization of free energy) of a slab, imposing VF's as external forces. This calculation was performed with five different slabs having the in-plane spacing expanded at the theoretical bulk value corresponding to $T=0$, 110, 300, 500, and 700 K. In order to check the accuracy of these results, we calculated a second set of VF's for $T=700$ K in the corresponding equilibrium positions. The new VF's were used to solve Eq. (3) again and the resulting relaxation did not change significantly. We conclude that, for this system, correct results can be obtained performing just one step in the self-consistent cycle described in Sec. II A to solve Eq. (2).

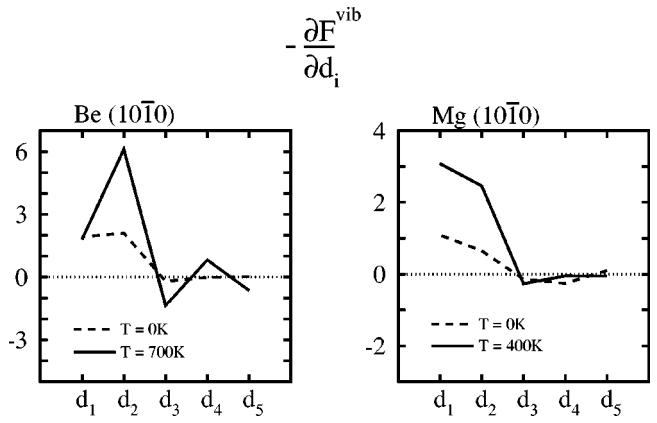

FIG. 2. Be$(10\bar{1}0)$ and Mg$(10\bar{1}0)$ surfaces: calculated derivatives of the vibrational free energy (of a 1×1 surface unit cell) with respect to displacements perpendicular to the surface for the five outermost layers (d_1, . . . d_5), at various temperatures. VF's with a positive sign lead to an expansion toward the vacuum. Units are Ry/Bohr.

VF's are shown in Fig. 2 and are compared with the VF's that we calculated in our work on the Mg$(10\bar{1}0)$ surface.[3] In both Be and Mg we calculated only the five outermost VF's, obtaining that the largest VF's are those on the two outermost layers. The other VF's are much smaller, indicating that five VF's are enough to obtain quantitatively correct results for the relaxation of the first four spacings. An interesting feature, appearing from Fig. 2, is that on Be$(10\bar{1}0)$ the VF of the second surface layer is larger and increases faster with temperature than the VF of the first layer. This means that, increasing the temperature, the entropic effect will ''push'' the second layer toward the vacuum more strongly than the first one. We can, thus, expect that the first surface interlayer will undergo thermal contraction. On the contrary, on the Mg$(10\bar{1}0)$ surface, the VF on the first layer is larger than the one on the second.

The different behavior of the VF's is not surprising given the fact that the phonon dispersion of the two surfaces are qualitatively different. In fact, the surface phonon dispersion of Be$(10\bar{1}0)$, analyzed in Ref. 23, is somewhat ''anomalous.'' As an example, the lowest phononic branch between the surface Brillouin-zone points $\bar{A}$ and $\bar{\Gamma}$ is localized on the second surface layer and not on the topmost, as it would be natural to expect in a free-electron-like metal, and as it happens in the Mg$(10\bar{1}0)$ surface.[28] The calculated thermal expansion of Be$(10\bar{1}0)$ is shown in Fig. 3. We find an *oscillatory thermal relaxation*: thermal contraction of the short-interlayer spacing (i.e. d_{12}, d_{34}) and expansion of the long-interlayer spacing (i.e. d_{23}, d_{45}). The same behavior, although weaker, was previously found in Mg$(10\bar{1}0)$.[3]

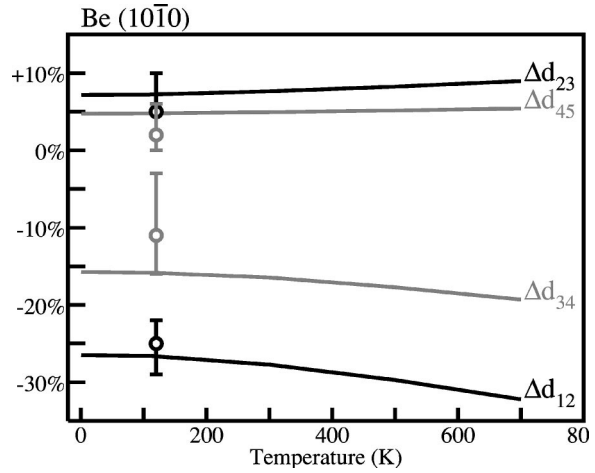

FIG. 3. Calculated thermal relaxation of Be(10$\bar{1}$0) surface. $\Delta d_{ij}(T)=[d_{ij}(T)-d_{ij}(0)]/d^{blk}(T)$, where d_{ij} is the distance between ith and jth surface layers, and $d^{blk}(T)$ is the corresponding bulk value at the temperature T. Open dots are LEED measurements from Ref. 24.

Moreover, as in Mg, the sum of a ''short'' and a ''long'' spacing ($d_{n,n+2}$) is less contracted and less dependent on temperature than single interlayer spacings ($d_{n,n+1}$). As two examples, Δd_{13} is -3.8% at $T=0$ K and reaches -4.2% at $T=700$ K, while Δd_{24} remains -0.5% from $T=0$ K up to $T=700$ K.

Finally, zero-temperature calculations of Fig. 3 are different from static-equilibrium results of Table I because of the inclusion of zero-point energy effects. The two results are very similar (within a couple of percents) because contributions from bulk zero-point energy and surface zero-point energy are nearly canceling each other. The first leads to an expansion of the bulk equilibrium lattice spacing,[7] which, in turn, leads to an overall contraction of the surface. The second, acting directly on the surface layers, leads to an overall expansion of the surface.

IV. DISCUSSION

We have shown that Be(10$\bar{1}$0) undergoes an oscillatory thermal relaxation similar to the one previously observed on Mg(10$\bar{1}$0).[3] In Sec. III B we suggested that the oscillatory relaxation at zero temperature is a consequence of the relative stiffness in the potential between different layers. In such a situation, an increased contraction of the first interlayer (d_{12}), as the temperature increases, will lead to the observed oscillatory thermal relaxation. In this section we will analyze the mechanism leading to d_{12} thermal contraction on Be and Mg(10$\bar{1}$0) surfaces.

A. Static and vibrational contribution

At finite temperature, the mean position of atomic surface layers is determined by the balance between energetic and entropic effects. The thermal relaxation of a surface is, thus, given by two main contributions. Due to the bulk thermal expansion, the in-plane lattice spacing of a surface increases with temperature, leading to a change of the static interlayer forces. We will refer to this as to the ''static'' contribution. The second contribution comes from the entropic term in the surface free energy, and will be called ''vibrational'' since is directly related to the surface VF's. Let us consider a surface having as in-plane lattice spacing, the lattice spacing $\mathbf{a}(T)$ of the bulk at the temperature T. Let us call $d_i^s(T)$ the static-equilibrium layer positions of this surface, that are the positions obtained by minimizing only the static energy. Since the surface free energy is not considered, the dependence of d_i^s on the temperature is solely due to what we called the ''static'' contribution. Let us now call $d_i^v(T)$ the relaxation obtained applying the surface VF's to the layers of a surface in which the in-plane lattice spacing is kept fixed at the $T=0$ value. The dependence of d_i^v on the temperature is solely due to what we called the ''vibrational'' contribution. Clearly, both contributions are present in a real system, and can be isolated only in an ideal experiment. Also, notice that the static-equilibrium positions described in Sec. III B) are different from $d_i^s(0)$, since in this last case the bulk lattice spacing is changed by zero-point energy.

A simple model to clarify these concepts is the following. Expanding the static energy up to the second order around d_i^s, Eq. (3) becomes

$$\sum_j \left.\frac{\partial^2 E}{\partial d_i \partial d_j}\right|_{\mathbf{a}(T),\mathbf{d}^s(T)} [d_j - d_j^s(T)] + \frac{\partial F^{vib}}{\partial d_i}[\mathbf{a}(T),\mathbf{d},T] = 0. \tag{18}$$

Furthermore, if we assume that the second derivative of the energy and the VF's do not depend on the structure of the system, Eq. (18) becomes

$$\sum_j \frac{\partial^2 E}{\partial d_i \partial d_j}[d_j - d_j^s(T)] + \frac{\partial F^{vib}}{\partial d_i}(T) = 0. \tag{19}$$

The solution of the system is, thus

$$d_i = d_i^s(T) - \sum_j \left(\frac{\partial^2 E}{\partial d \partial d}\right)^{-1}_{ij} \frac{\partial F^{vib}}{\partial d_j}(T)$$

$$= d_i^s(T) + \delta d_i^v(T) = d_i^0 + \delta d_i^s(T) + \delta d_i^v(T), \tag{20}$$

where d_i^0 are the layer positions at zero temperature. This approach is not an oversimplified one. Indeed, we could show that it produces quantitatively correct results for Be and Mg(10$\bar{1}$0) surfaces. However, the main reason we discuss it is that, in this model, the thermal relaxation is given exactly by the sum of two distinct contributions. By definition, the dependence of δd_i^s on T is purely ''static.'' On the other hand, the dependence of δd_i^v on T is purely ''vibrational,'' and it can be easily verified that with this model $d_i^v(T)=d_i^0+\delta d_i^v(T)$. This model should, thus, help the reader to understand how the two contribution that we called ''static'' and ''vibrational'' affect the surface thermal expansion.

It is well known that a crystal described by a purely harmonic interatomic potential does not undergo thermal expansion. However, the fact that in the described model the static

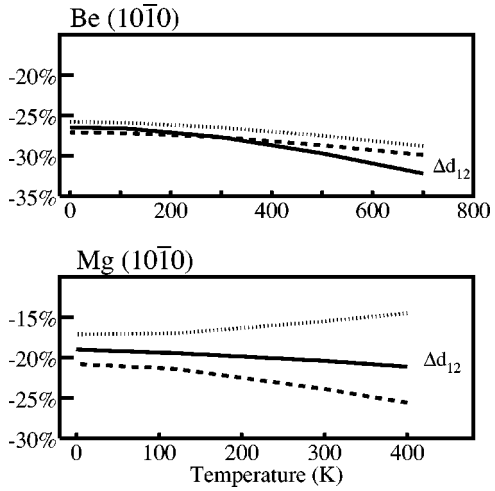

FIG. 4. Be(10$\bar{1}$0) and Mg(10$\bar{1}$0) surfaces: thermal relaxation of the distance between the first two surface layers. Continuous lines show the actual thermal relaxation. Dashed (dotted) lines are obtained from $d_i^s(T)$ [$d_i^v(T)$], defined in the text, and represent the ''static'' (''vibrational'') contribution to the thermal expansion.

energy is harmonic is not contradictory. Indeed, if the anharmonic terms of the static energy are sufficiently small it can be shown that in Eq. (1) the static energy can be considered harmonic introducing only a negligible error. On the contrary, the dependence of F^{vib} on the anharmonic terms is essential for thermal expansion to occur.

B. Be, Mg(10$\bar{1}$0), and Al(110): A comparison

In order to understand how the ''static'' and ''vibrational'' contributions influence the first interlayer thermal contraction we calculated the $d_i^s(T)$ and $d_i^v(T)$, defined in the preceding section for both Be and Mg(10$\bar{1}$0) surfaces. The results for the first interlayer distance are shown in Fig. 4. We observe that the ''static'' relaxation leads to a contraction of d_{12}, by increasing T, both in Be and Mg. Actually, if surface vibrational contributions are not taken into account, it is hardly surprising that by increasing the in-plane lattice spacing the first surface interlayer distance contracts, so as to keep the atomic volume nearly constant. The relaxation due to the ''vibrational'' contribution in Be and Mg is instead different. In the case of Mg it leads to an expansion, thus behaving in a rather ''normal'' way, while in Be it leads to a contraction by increasing T. This behavior can be related to the already noticed difference of the VF's in the two surfaces. In Be the VF on the second layer increases faster with temperature than the VF on the first layer, favoring d_{12} contraction. On the contrary, in Mg the VF on the first layer increases faster than the one on the second layer, favoring d_{12} expansion. In summary, d_{12} thermal contraction occurs in both Be and Mg(10$\bar{1}$0) surfaces but, while in Mg(10$\bar{1}$0) it is due to the ''static'' contribution, which is actually nearly compensated by the ''vibrational'' one, in Be(10$\bar{1}$0) both the ''static'' and the ''vibrational'' contributions are leading to thermal contraction and a stronger effect is predicted in this case.

Finally, d_{12} thermal contraction had been observed also in Al(110) surface.[1,2] In this case, after analyzing the results of a molecular-dynamic simulation, the authors of Ref. 2 argue that the observed thermal contraction is a consequence of the larger anharmonicity of the second surface layer with respect to the first one. Indeed, a measure of the anharmonicity of a degree of freedom is the corresponding VF and we find that one important contribution to thermal contraction in Be(10$\bar{1}$0) surface occurs because the VF on the second layer is larger than the VF on the first one, that is, the anharmonicity in the second layer is stronger than in the first one. Thus, it seems that there is a rather strict analogy between the thermal contraction in Al(110) and Be(10$\bar{1}$0) surfaces. On the other hand, in Mg(10$\bar{1}$0) surface thermal contraction is weaker and somehow accidental, resulting from the delicate balance of the ''static'' and ''vibrational'' contributions in this system.

V. CONCLUSIONS

In this work we developed a method for the efficient computation of the third-order derivative of the total energy in a metallic system, thanks to the ''$2n+1$'' theorem and using the density-functional perturbation theory. The implementation of the method allowed us to study, within the quasiharmonic approximation, the thermal expansion of systems described by many structural parameters. As an application we presented a study of the thermal expansion of Be(10$\bar{1}$0) surface. Increasing the temperature the surface undergoes a remarkable *oscillatory thermal relaxation* similar to and stronger than the one previously calculated and observed in Mg(10$\bar{1}$0) surface. We suggest that this phenomenon is due to the thermal contraction of the first interlayer distance propagating to the lower layers in an oscillatory way because of the relative stiffness of the potentials between different layers. According to our analysis, in Mg(10$\bar{1}$0) the first interlayer thermal contraction results from a delicate balance between two opposite contributions. While the change in surface static forces, caused by the bulk thermal expansion, favors contraction, the VF's tend to make the first interlayer distance expand. On the contrary, in Be(10$\bar{1}$0), the large anharmonicity of the second surface layer plays an important role in enhancing the thermal contraction and the resulting effect is much stronger.

ACKNOWLEDGMENTS

We are grateful to N. Marzari, Ismail, and S. Narasimhan for helpful discussion. Part of the work was done within the *Iniziativa Calcolo Parallelo* of INFM, and we acknowledge partial support from COFIN program of MIUR. All calculations were performed employing the PWSCF and PHONON packages.[18] The codes we implemented for the present work are available on the web, at the same URL.[18]

*Present address: Laboratoire de Minéralogie et Cristallographie de Paris, UMR CNRS 7590, Université Paris VI, 4 Place Jussieu, 75252 Paris Cedex 05, France.

[1] A. Mikkelsen, J. Jiruse, and D.L. Adams, Phys. Rev. B **60**, 7796 (1999); B.W. Busch and T. Gustafsson, *ibid.* **61**, 16 097 (2000).
[2] N. Marzari, D. Vanderbilt, A. De Vita, and M.C. Payne, Phys. Rev. Lett. **82**, 3296 (1999).
[3] Ismail, E.W. Plummer, M. Lazzeri, and S. de Gironcoli, Phys. Rev. B **63**, 233401 (2001).
[4] C.S. Jayanthi, E. Tosatti, and L. Pietronero, Phys. Rev. B **31**, 3456 (1985).
[5] P. Hohenberg and W. Kohn, Phys. Rev. **136**, B864 (1964); W. Kohn and L.J. Sham, *ibid.* **140**, A1133 (1965).
[6] S. Narasimhan and M. Scheffler, Z. Phys. Chem. (Munich) **202**, 253 (1997); J.H. Cho and M. Scheffler, Phys. Rev. Lett. **78**, 1299 (1997).
[7] M. Lazzeri and S. de Gironcoli, Phys. Rev. Lett. **81**, 2096 (1998).
[8] J.J. Xie, S. de Gironcoli, S. Baroni, and M. Scheffler, Phys. Rev. B **59**, 970 (1999).
[9] A. Kara, P. Staikov, A.N. Al-Rawi, and T.S. Rahman, Phys. Rev. B **55**, 13 440 (1997).
[10] U. Hansen, P. Vogl, and V. Fiorentini, Phys. Rev. B **60**, 5055 (1999).
[11] A.N. Al-Rawi, A. Kara, P. Staikov, C. Ghosh, and T.S. Rahman, Phys. Rev. Lett. **86**, 2074 (2001).
[12] S. Baroni, P. Giannozzi, and A. Testa, Phys. Rev. Lett. **58**, 1861 (1987); S. Baroni, S. de Gironcoli, A. Dal Corso, and P. Giannozzi, Rev. Mod. Phys. **73**, 515 (2001).
[13] X. Gonze and J.P. Vigneron, Phys. Rev. B **39**, 13 120 (1989).
[14] S. de Gironcoli, Phys. Rev. B **51**, 6773 (1995).
[15] A. Debernardi and S. Baroni, Solid State Commun. **91**, 813 (1994).
[16] A. Dal Corso and F. Mauri, Phys. Rev. B **50**, 5756 (1994).
[17] M. Methfessel and A.T. Paxton, Phys. Rev. B **40**, 3616 (1989).
[18] S. Baroni, A. Dal Corso, S. de Gironcoli, and P. Giannozzi, http://www.pwscf.org
[19] D.M. Ceperley and B.J. Alder, Phys. Rev. Lett. **45**, 566 (1980); as parametrized by J.P. Perdew and A. Zunger, Phys. Rev. B **23**, 5048 (1981).
[20] L. Kleiman and D.M. Bylander, Phys. Rev. Lett. **48**, 1425 (1982).
[21] S.G. Louie, S. Froyen, and M.L. Cohen, Phys. Rev. B **26**, 1738 (1982).
[22] M. Lazzeri and S. de Gironcoli, Surf. Sci. **402-404**, 715 (1998).
[23] M. Lazzeri and S. de Gironcoli, Surf. Sci. **454-456**, 442 (2000).
[24] Ph. Hofmann, K. Pohl, R. Stumpf, and E.W. Plummer, Phys. Rev. B **53**, 13 715 (1996).
[25] J.H. Cho, K.S. Kim, S.H. Lee, M.H. Kang, and Z. Zhang, Phys. Rev. B **61**, 9975 (2000).
[26] S. Narasimhan, Phys. Rev. B **64**, 125409 (2001).
[27] M.W. Finnis and V. Heine, J. Phys. F: Met. Phys. **4**, L37 (1974).
[28] M. Lazzeri, Ph. D. thesis, SISSA-ISAS, 1999. Available at http://www.sissa.it/cm/PHD.html